

Numerical studies on timing response and efficiency of RPC

A. Jash^{a,c,1}, N. Majumdar^{a,c}, S. Mukhopadhyay^{a,c}, S. Chattopadhyay^{b,c}

^a*Applied Nuclear Physics Division, Saha Institute of Nuclear Physics, Block AF, Sector 1, Bidhannagar, Kolkata 700064, INDIA*

^b*Experimental High Energy Physics Division, Variable Energy Cyclotron Centre, Block AF, Sector 1, Bidhannagar, Kolkata 700064, INDIA*

^c*HBNI, Training School Complex, Anushakti Nagar, Mumbai 400094, INDIA*

Abstract

A detailed numerical simulation has been performed to investigate the timing properties of a standard bakelite RPC in order to optimize its application in INO-ICAL experiment designed for studying atmospheric neutrinos. The timing information provided by the RPC is an important observable in the experiment to determine the direction of the neutrinos. Effects of various operating conditions and design components on the RPC timing response, mainly the average signal arrival time and the time resolution have been studied in this context. The same properties have been simulated in case of a glass RPC and then compared to the measured values to validate the simulation method. The dependence of the detector efficiency on various operating and design parameters has also been found out.

1 Introduction

Resistive Plate Chamber (RPC) [1] has been chosen as the active detector element for the magnetized Iron CALorimeter (ICAL) setup [2] of 50 kTon target mass in the proposed underground laboratory facility of India-based Neutrino Observatory (INO). The ICAL has been designed for detecting the muons propagating through the calorimeter, identification of their charges and accurate determination of their energies and directions. These will allow for a sensitivity to the neutrino mass hierarchy and precision measurement of the neutrino mixing parameters. To accomplish the task, the ICAL will be equipped with RPCs stacked in horizontal layers interleaving 151 layers of iron plates of thickness 5.6 cm which will be magnetized to produce a uniform magnetic field of 1.3 T over the entire plate thickness. Muons of opposite charges (μ^- , μ^+) produced by the charged current (CC) interaction of incoming atmospheric muon neutrinos (ν_μ , $\bar{\nu}_\mu$) with the iron nuclei in the target mass will bend differently under the action of the magnetic field and their path will be tracked using the two dimensional position information provided by each RPC layer. In addition,

¹Corresponding author: abhik.jash@niser.ac.in

Present address: School of Physical Sciences, National Institute of Science Education and Research (NISER) Bhubaneswar, Khurda Road, 752050, INDIA.

the timing response of the RPCs will allow for a determination of directionality of the muons by distinguishing between up-going and down-going muons. All these measurements will allow to probe several important observables, such as, the earth-matter effect of ν_μ and $\bar{\nu}_\mu$ that travel through the earth before reaching the ICAL, their path length and the momenta. Fast timing response with time resolution of the order of one nanosecond and position resolution of the order of one centimeter from each detector layer are the basic requirements to achieve these goals.

A thorough understanding of the operation of RPC and dependence of its performance on different conditions will help us to optimize its application in the ICAL as well as interpret and predict the experimental results. The RPC made up of float glass electrodes has been opted for muon detection in ICAL. However, a simultaneous R&D has been underway to investigate the feasibility of using bakelite electrodes which can offer several advantages like high rate capability, easy handling and fabrication and can be an alternative option for the ICAL. In the present work, a detailed numerical simulation has been performed for this purpose to investigate the dynamics of a bakelite RPC for different operational as well as geometrical parameters which may be useful for validating its choice. Also, the numerical method has been used to predict the behavior of the detector at conditions which are difficult to realize using experiments. In this context, computation of the entire working procedure of an RPC beginning from the primary ionization caused by the passage of muons through it, till the generation of signal on its read-outs, has been performed using a simulation framework developed for the gaseous detectors. The main thrust has been put on the investigation of its timing performance under various conditions. A straightforward approach based on the basic principles of electronic signal detection has been implemented to calculate the timing response in the process of simulating the induced current signal. The same simulation has been performed for computing the timing properties of the glass RPC for which experimental data are available [3] to compare with the numerical work.

The content of the paper has been arranged in the following manner. The scheme of numerical simulation adopted to calculate the RPC response has been described in section 2. In section 3 the simulated results for a glass RPC has been compared with the available experimental data. The effect of different operating conditions and the geometrical components on the timing properties and the efficiency of a bakelite RPC has been presented in section 4. The computer resources used for the present simulation work have been mentioned in section 5. Finally, concluding remarks are made in section 6.

2 Simulation scheme

RPC being a gaseous detector, works on the principle of ionization phenomenon caused by the passage of a charged particle/radiation through its gaseous volume. When an energetic charged particle or radiation passes through the gaseous medium, it imparts its energy partially to the molecules of the gas mixture, causing their ionization or excitation. In presence of the electric field, the electrons and cations, created in the primary ionization, move towards the anode and the cathode, respectively. At lower values of the electric field, the electrons and cations may get lost due to processes like recombination, attachment, electron capture etc. When the electric field is sufficiently high, the primary electrons may gain enough kinetic energy to ionize other molecules when they collide with

them, liberating more electrons and cations. Depending upon the kinetic energy gathered by the primaries, they can cause further ionization even after the secondary level. On the other hand, the cations, being very heavy, generally move slower and the probability of secondary ionization by the cations is quite less usually. The movement of all the ions, thus produced in a cascade of ionization, commonly called as avalanche, induces a current on the conductive read-out panel. Following the Shockley-Ramo theorem [4, 5], the current induced by a charge q , moving with an instantaneous velocity $\vec{v}(t)$, is given by the equation 1:

$$i(t) = q \vec{v}(t) \cdot \vec{W}(\vec{x}(t)) \quad (1)$$

where, $\vec{W}(\vec{x}(t))$ is the weighting field for a read-out and that is calculated as the electric field produced at the instantaneous position ($\vec{x}(t)$) of the charge (q) when the read-out of interest is kept at unit potential while all other available conductors are grounded. The signal thus collected from the read-out strips is the characteristic response of the RPC that depends on its geometry, electric field and the filling gas mixture for a given incident particle or radiation. In the present work, the timing properties of a bakelite RPC have been studied for variation in its operational parameters, such as, supplied voltage and filling gas mixture. In addition, the effect of geometrical components, such as, the edge and the button spacer has been investigated as well. To accomplish these, numerical simulation of the RPC signal for different operational and geometrical conditions has been performed by calculating the current induced on one of its read-out strips using Garfield [6]. Garfield is a simulation framework which has interfaces to several toolkits, namely, HEED [7], neBEM [8], Magboltz [9], to compute different auxiliary components relevant to the gaseous detector dynamics, such as, primary ionization, electrostatic field, transport properties of the gas respectively. The final stage of signal calculation is computed by the Garfield with the use of relevant data produced by the respective toolkits.

The information on the primary ionization in the RPC gas chamber filled with a given gas mixture due to the passage of a muon with a specific energy and direction can be obtained using HEED. As an example, figure 1(a) shows a distribution of number of primary electrons generated per event by the passage of 5000 muons each of energy 2 GeV traveling in a fixed direction (5° with respect to the zenith) through a 2 mm gas gap containing $C_2H_2F_4$, 5% $i-C_4H_{10}$ and different fractions of SF_6 . Landau fit of the distribution produces a most probable value (MPV) of 34.81 denoting a primary electron density of 174.05/cm for the given gas mixture. Figure 1(b) shows the spatial distribution of the primary electrons along the thickness of the gas gap which indicates an almost uniform probability for ionization across the entire gap. No significant effect on the primary ionization properties has been found for varying the SF_6 fraction from 0.0% to 0.5%.

In simulating the detector response, it is important to carry out a precise computation of the field configuration within the detector because it plays the principal role in the detector dynamics. The detail electrostatic field map within a 30 cm \times 30 cm bakelite RPC has been calculated using two numerical methods, namely, finite element method (COMSOL Multiphysics[®] [10]) and boundary element method (neBEM [8]) and the results are available in [11]. For the present work, the field map has been calculated using neBEM v1.8.20. The same calculation has been repeated for glass RPC using a different relative dielectric constant, $\epsilon_r = 13.5$, for the glass electrodes in geometry. The time dependence of the electric

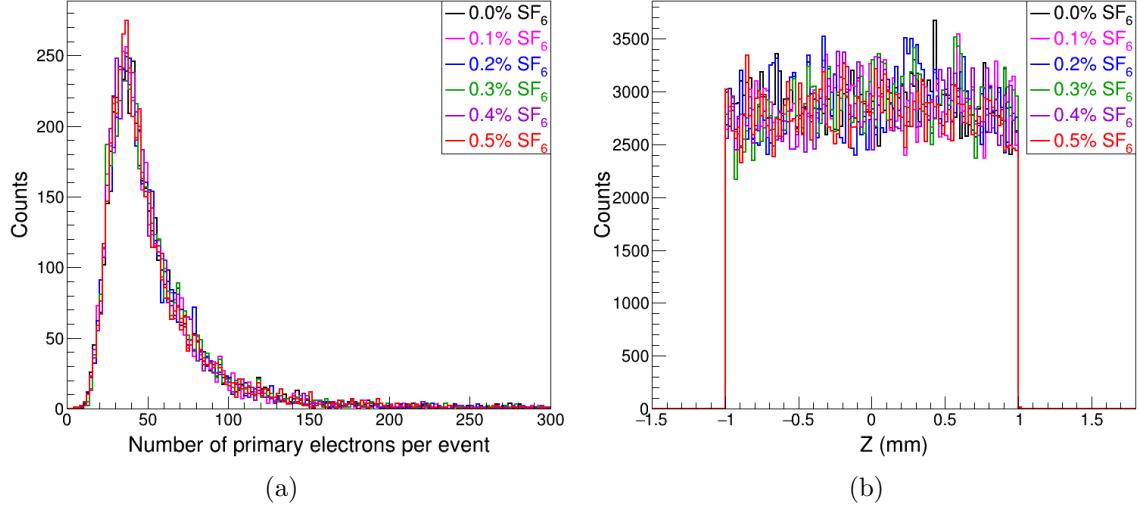


Figure 1: (a) Distribution of number of primary electrons per event and (b) spatial distribution of primaries in a 2 mm gas gap when 5000 mono-energetic muons, each of energy 2 GeV traveling in the same direction pass through the chamber containing the mixture C₂H₂F₄, 5% i-C₄H₁₀ and different fractions of SF₆.

field owing to the finite bulk resistivity of the RPC plate has been ignored as it is not expected to affect the signal [12]. An appropriate approach for this study would be to find out the signal in the presence of a dynamic electric field as the space charges created in the avalanche process tend to modify it [13]. However, the calculations in the present work have been performed assuming a static electric field configuration where the RPC is described as a multi-dielectric planar capacitor.

The electron transport properties in different gas mixtures have been calculated using the standalone Magboltz v8.9.3 program for different field values. The variation of the electron transport properties, such as, effective Townsend coefficient ($\alpha_{eff} = \alpha - \eta$) which is the value after subtracting the attachment coefficient (η) from the first Townsend coefficient (α), drift velocity (V_z) and longitudinal (D_l) and transverse (D_t) diffusion coefficients have been calculated for C₂H₂F₄ based gas mixtures containing 5% i-C₄H₁₀ and a small fraction of SF₆ that varies between 0.0 - 0.5%. The results are shown in figure 2 and 3. It can be seen from figure 2(a) that with the increase in applied field, the effective Townsend coefficient increases signifying more ionizations and less attachment of electrons for any given mixture. It reduces at a given field value when the amount of SF₆ is increased in the mixture for the obvious reason that SF₆ has a great affinity of electrons. In figure 2(b), the drift velocity of electrons increases with the field which makes the detector response faster. However, there is no effect of changing SF₆ fraction observed on this parameter. Figure 3(a) and 3(b) displays the variation of longitudinal and transverse diffusion coefficients with the applied electric field. In case of longitudinal diffusion, a rising trend in the coefficient with the increase in the field has been observed. On the other hand, the transverse diffusion coefficient shows a rise upto a field value of about 40 kV/cm and a subsequent fall. The variation in SF₆ fraction causes a very little change in both the diffusion coefficients.

The signal induced on a RPC read-out strip has been calculated by passing muons of energy randomly varying between 0.5 - 10 GeV through the detector

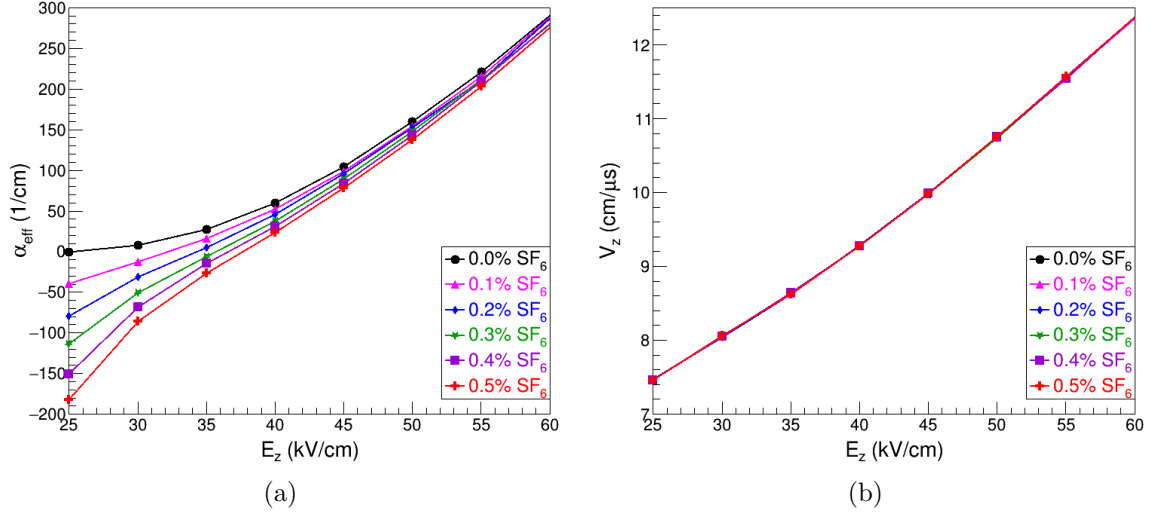


Figure 2: Variation of (a) effective Townsend coefficient (α_{eff}) and (b) drift velocity of electrons (V_z) with the applied field (E_z) for different fractions of SF_6 in the gas mixture $C_2H_2F_4 + 5\% i-C_4H_{10} + SF_6$.

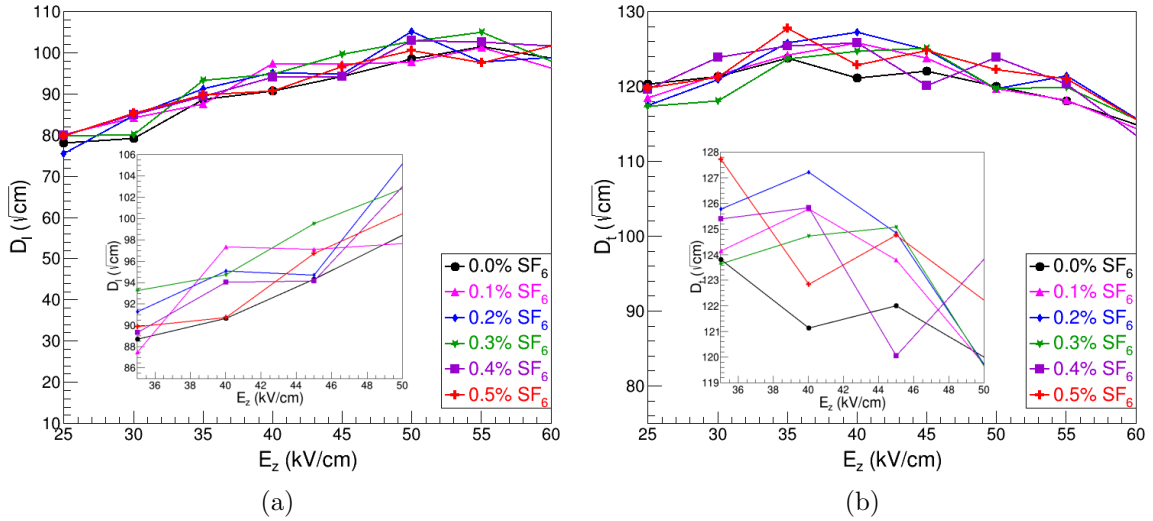


Figure 3: Variation of (a) longitudinal (D_l) and (b) transverse (D_t) diffusion coefficients of electrons with the applied field (E_z) for different fractions of SF_6 in the gas mixture $C_2H_2F_4 + 5\% i-C_4H_{10} + SF_6$ (insets of both figures contain the variations in a shorter scale).

in randomly varying directions restricting the incidence angle (θ) within $0^\circ - 10^\circ$. The movement of all the electrons and ions created in the gas mixture through the avalanche process has been tracked by the Garfield and the current induced on the pickup strip due to their movement has been calculated at an interval of 100 ps. A typical signal shape as found from numerical calculation is shown in figure 4(a). The experimentally obtained signal shapes generally appear with a long tail which is absent in the simulated current signal. This can be attributed to the assumption of simplified ion movement and non-inclusion of the effect of the electronics and the detector components outside the gas chamber. The positive ions, having a larger mass and contributing to the slower falling edge, have been treated as moving with a constant velocity and not contributing to

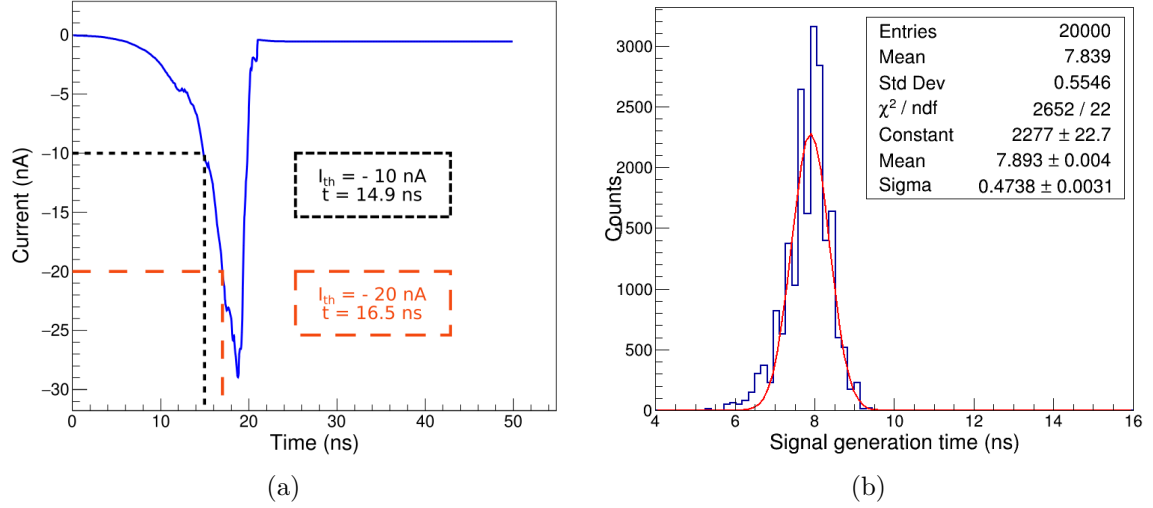


Figure 4: (a) A typical simulated RPC signal and the scheme of selecting signal generation time corresponding to crossing different set thresholds, (b) distribution of signal generation times for 2000 events and its fit with Gaussian function for an RPC operated with $\text{C}_2\text{H}_2\text{F}_4$, 5% $\text{i-C}_4\text{H}_{10}$ and 0.2% SF_6 at 42 kV/cm (used threshold = 10 nA).

the growth of avalanche. The computed signal shapes have been analysed using Root data analysis framework [14] to find the timing properties of the detector. A threshold in the current value has been used in the simulation for eliminating the low amplitude noise signals as is usually done in experiments. The selection of times corresponding to crossing two fixed values of current thresholds are indicated in figure 4(a). The time corresponding to crossing a specific threshold has been defined as the signal generation time. A distribution of the signal generation times has been obtained for 2000 events where each event represents an averaging of current signals of 10 muons of randomly varying energy and angle of incidence within the mentioned range. A typical distribution of signal generation times, to cross a threshold of 10 nA current, is shown in figure 4(b). The distribution has been fit with a Gaussian function to obtain the average signal generation time and the intrinsic time resolution of the detector from its mean and standard deviation, respectively.

The amplitude of the induced signals has been calculated for 2000 events (20000 muons with randomly varying energy and direction as mentioned earlier). A distribution of signal amplitudes has been thus obtained for each set of applied field and gas mixture. One of such distributions when the RPC has been operated at a field of 42 kV/cm and with a gas mixture of 94.8% $\text{C}_2\text{H}_2\text{F}_4$, 5% $\text{i-C}_4\text{H}_{10}$ and 0.2% SF_6 is shown in figure 5(a). The mean of the distribution, termed as average signal amplitude, has been used to denote the characteristic response at different operating conditions. To study the effect of the applied field and the SF_6 content in the gas mixture on the detector efficiency, the average signal amplitudes have been calculated for different field values with a gas mixture of $\text{C}_2\text{H}_2\text{F}_4$, 5% $\text{i-C}_4\text{H}_{10}$ and different percentages of SF_6 varying from 0 to 0.5%. The average signal amplitude were found to increase at higher electric field and for lower SF_6 in the gas mixture (figure 5(b)). At higher fields the rise in the Townsend coefficient or the gain in kinetic energy of the electrons caused release of larger number of electrons through further ionization of the gaseous molecules

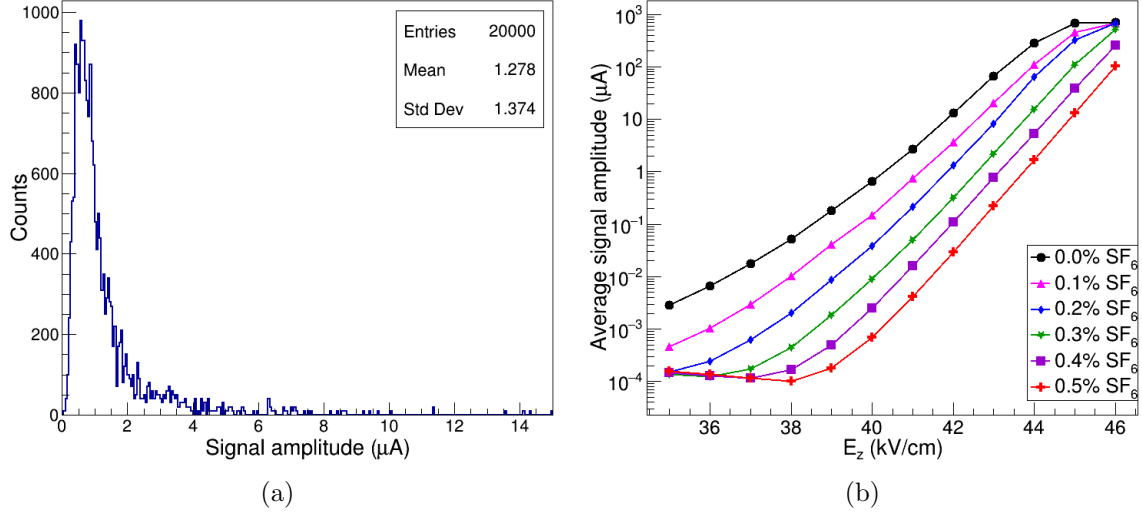


Figure 5: (a) Distribution of signal amplitudes from a RPC operated with $\text{C}_2\text{H}_2\text{F}_4$, 5% $\text{i-C}_4\text{H}_{10}$ and 0.2% SF_6 at 42 kV/cm , (b) variation of average signal amplitude with the applied field for different fractions of SF_6 in the gas mixture, containing 5% $\text{i-C}_4\text{H}_{10}$ and rest $\text{C}_2\text{H}_2\text{F}_4$.

that contributed to the rise in the induced current. On the other hand, the effect of addition of a trace amount of highly electronegative SF_6 in the gas mixture caused a reduction in the signal amplitude owing to attachment of electrons with the SF_6 molecules. Addition of SF_6 to the gas mixture is necessary to restrict streamer generation which may deteriorate the detector performance. The detector efficiency has been calculated by finding out the fraction of events which has been able to generate a signal amplitude more than a specified threshold.

3 Comparison of numerical and experimental data

Experimental results for variation of the timing parameters with the fraction of SF_6 for a glass RPC of size $2\text{ m} \times 2\text{ m}$ is available in [3]. Numerical calculations have been done for the same prototype with smaller lateral dimension ($16\text{ cm} \times 16\text{ cm}$) using the dielectric constant of Asahi glass [15] for field calculation. The average signal generation time and intrinsic time resolution of the RPC has been calculated at different applied fields for gas mixtures containing different fractions of SF_6 . The variation of average signal arrival time and intrinsic time resolution of the glass RPC with applied field is shown in figure 6. Both the parameters have been found to reduce with the increasing field. Effect of SF_6 on the parameters is also evident from figure 6. Presence of SF_6 has been found to deteriorate the timing performance. The effect is more prominent at lower field values and tend to vanish at a higher fields.

In the experiments [3], both the timing parameters were found to deteriorate with the increase in SF_6 fraction in the gas mixture. The variation of the two timing parameters with the fraction of SF_6 has been found out from the numerical data and compared with the experimental result in figure 7 and 8. It can be noticed from figure 6 that the nature of variation of the timing parameters on the SF_6 fraction depends on the chosen value of E_z . The dependence

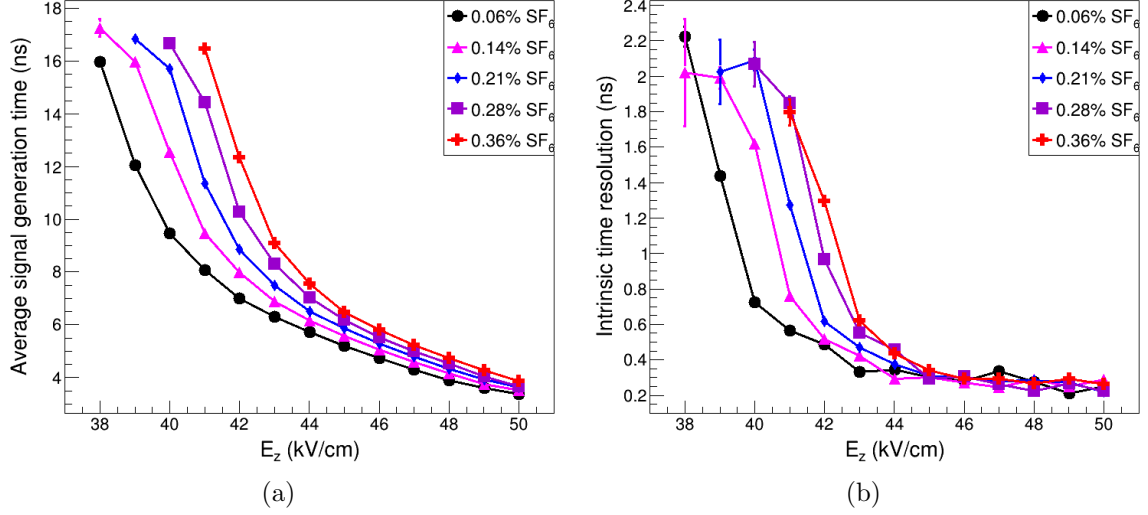


Figure 6: Variation of (a) average signal generation time and (b) intrinsic time resolution of a glass RPC with the applied field for different fractions of SF_6 present in the gas mixture.

of the intrinsic time resolution on the SF_6 fraction seem to vanish after around 45 kV/cm. The simulated values of signal generation time and intrinsic time resolution are much small in magnitude than the experimental values which is normal as the simulation is done by considering only the activities within the gas volume. The delay and the jitter introduced by the electronic components and connecting wires are not present in it. The value of the time delay, added to the signal generation time and the jitter, added in quadrature to the intrinsic time resolution, has been adjusted for the simulated values at different applied fields to find the best match between the experimental data and the simulated results. In the process, it had not been possible to find a particular electric field for which the variation of both the timing parameters with SF_6 fraction from numerical calculation matches with that from experiment. In figure 7 the simulated results at $E_z = 44.05$ kV/cm has been compared with the experimental data to get best match for the arrival time after adding a delay of 54.12 ns with the simulated signal generation time. But in the same condition, the time resolution curve obtained from simulation after adding a jitter of 1.4 ns does not follow the trend as found in the experiment. It has been possible to match the trend of the time resolution curve by selecting the simulated data for $E_z = 42.15$ kV/cm and a jitter of 1.26 ns. The comparison plot is shown in figure 8(b). The curve for the signal arrival time in the same condition with an additional delay of 51.7 ns has been compared in figure 8(a).

The difficulty in matching both the simulated timing parameters simultaneously with the experimental data can be attributed to the following factors. In the experiments, controlling the fraction of SF_6 flow to very small value needs special Mass Flow Controllers (MFCs) and is difficult to maintain which can be a possible source of error. The numerical calculations does not consider any effect of streamer whereas the fraction of SF_6 strongly influences the streamer production in the gas. However, from all the plots it is evident that the presence of SF_6 worsens the timing properties of the detector.

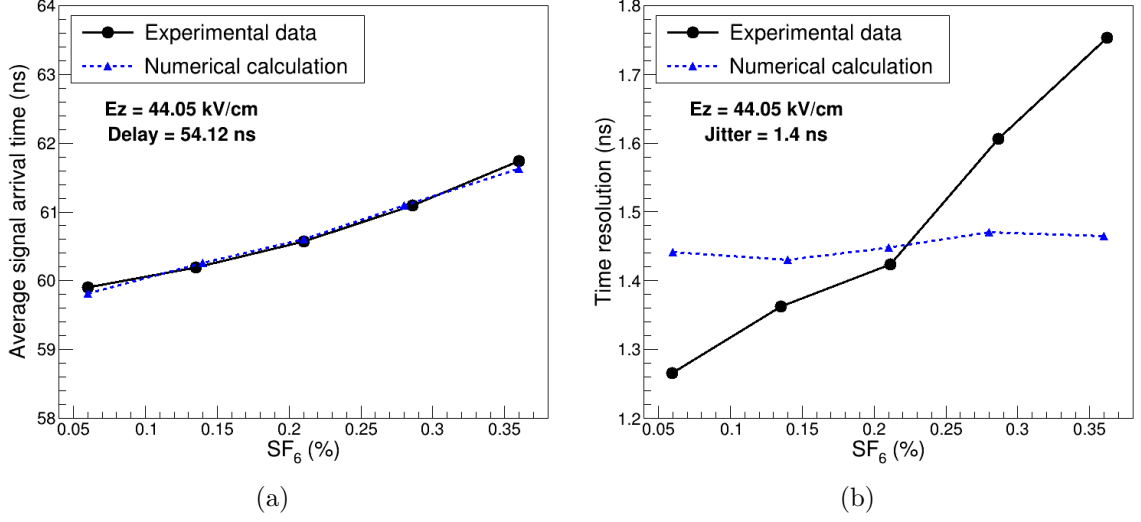


Figure 7: Comparison of experimental and simulated results for the variation of (a) average signal arrival time and (b) time resolution of a glass RPC with the fraction of SF₆ present in the gas mixture (experimental data from [3], simulation results at E_z = 44.05 kV/cm, delay = 54.12 ns added to the signal generation time and jitter = 1.4 ns added to the intrinsic time resolution). Statistical errors in the data points from numerical calculation are within marker sizes.

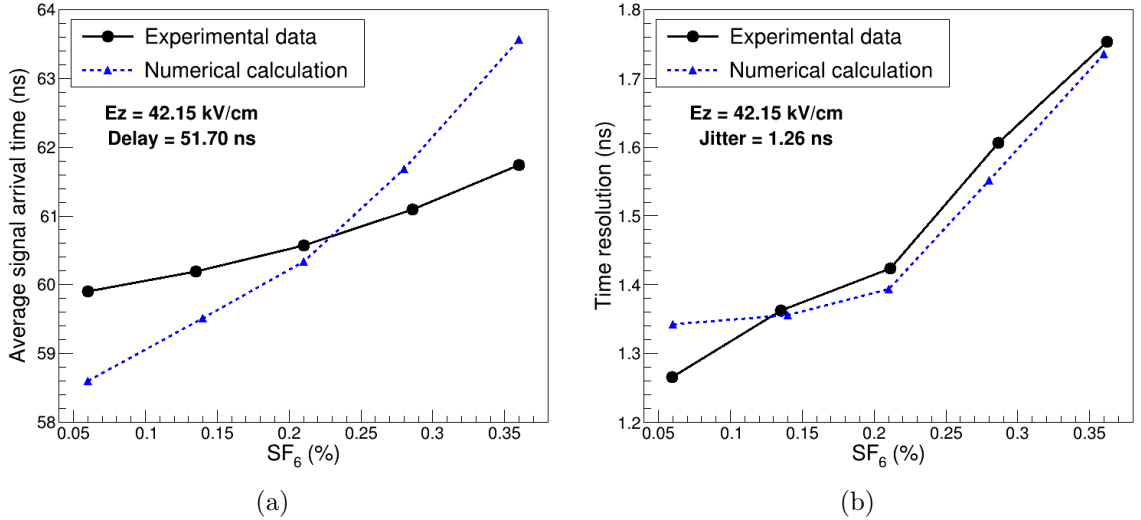


Figure 8: Comparison of experimental and simulated results for the variation of (a) average signal arrival time and (b) time resolution of a glass RPC with the fraction of SF₆ present in the gas mixture (experimental data from [3]), simulation results at E_z = 42.15 kV/cm, delay = 51.70 ns added to the signal generation time and jitter = 1.26 ns added to the intrinsic time resolution). Statistical errors in the data points from numerical calculation are within marker sizes.

4 Numerical results

4.1 Effect of operational parameters

Figure 9 shows the variation of average signal generation time and intrinsic time resolution of RPC with the applied field when the RPC is operated with gas mix-

tures containing different fractions of SF_6 along with $\text{C}_2\text{H}_2\text{F}_4$ and 5% $\text{i-C}_4\text{H}_{10}$. The curves have been obtained by setting a threshold of 10 nA. Values of both

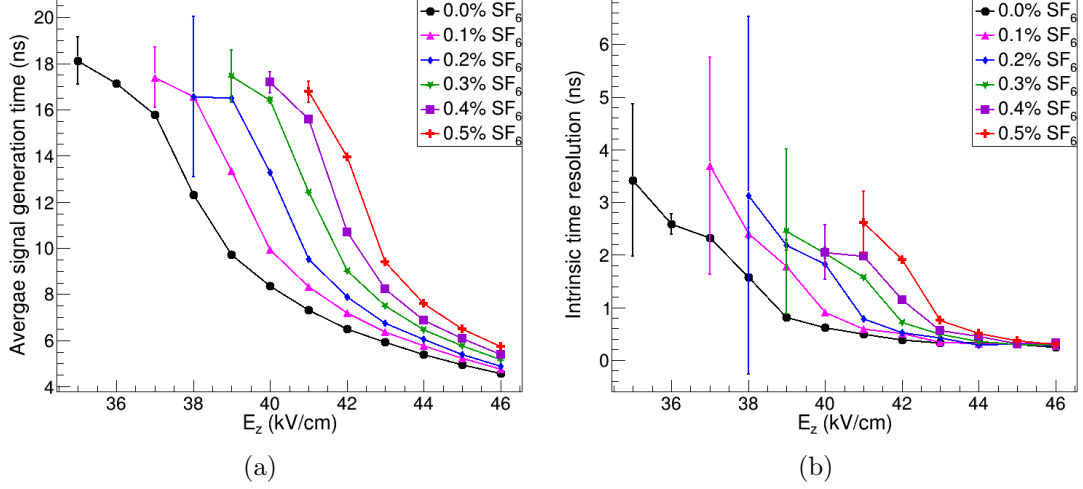


Figure 9: Variation of (a) average signal generation time and (b) intrinsic time resolution of a bakelite RPC with the applied field for different fraction of SF_6 content in the used gas mixture ($\text{C}_2\text{H}_2\text{F}_4 + 5\% \text{i-C}_4\text{H}_{10} + \text{SF}_6$) when the set threshold is 10 nA.

the timing parameters have been found to decrease at higher fields implying a better timing performance of the detector. At higher values of field avalanche multiplication is larger which produces the detectable signal earlier and in turn reduces the average signal generation time; the increase of both the effective Townsend coefficient and drift velocity of electrons at higher field region (refer to figure 2) is responsible for the improvement of the time resolution according to the analytic formula described in [16]. The effect of streamer quenching component of the gas mixture *i.e.* SF_6 on the timing properties is also evident from figure 9. The timing performance deteriorates for the gas mixtures containing higher fraction of SF_6 . The difference in the values for the two timing parameters for different gas mixtures is prominent at lower field values which diminishes at higher values of the field.

The value of the timing parameters has been found to depend on the used threshold also. Variation of the two timing parameters with the used threshold has been shown in figure 10 for two different fields and gas mixtures containing different fractions of SF_6 . Again in this case, the dependence of the timing parameters on the used threshold has been found to be more prominent for lower field values and with higher fraction of SF_6 in the gas mixture.

The variation of the detector efficiency with the applied field for different fractions of SF_6 in the gas mixture is shown in figure 11(a) for crossing a threshold of 10 nA. The efficiency increased with the applied field and reached a plateau (100% efficiency) after a while. For higher fraction of SF_6 in the gas mixture, a comparatively higher value of field is required to reach the plateau region. The effect of used set threshold on the detector efficiency can be found out from figure 11(b) where variation of detector efficiency with the used threshold has been shown for two different field values and two different fractions of SF_6 in the gas mixture. For lower values of field and moderate amount of SF_6 , the detector efficiency has been found to get reduced at higher threshold values as some of the events could not produce signals crossing the set threshold. For higher field values and without inclusion of SF_6 the signal production is very efficient and

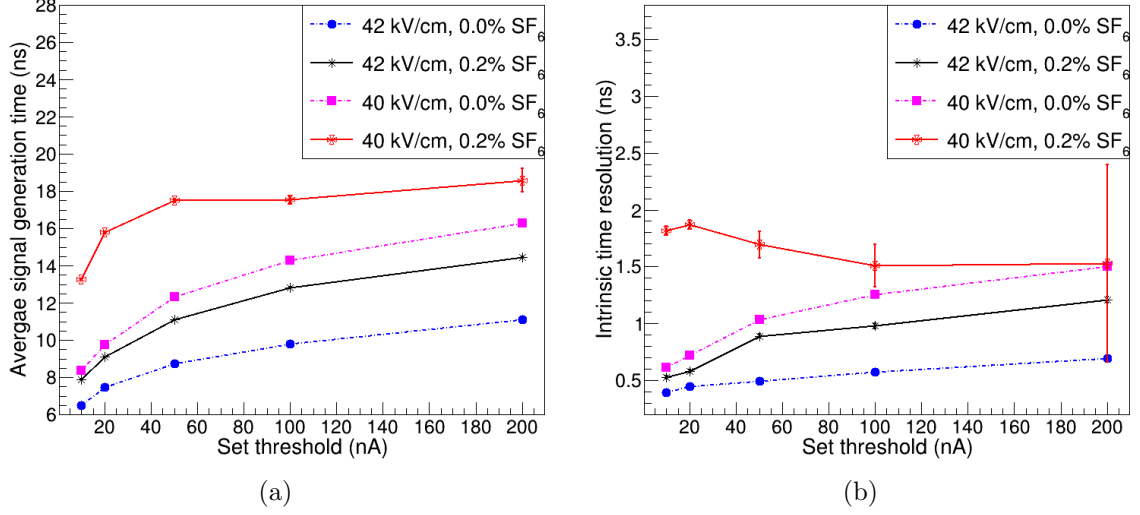


Figure 10: Variation of (a) average signal generation time and (b) intrinsic time resolution of a bakelite RPC with the used threshold for different gas mixtures operated in presence of different field values.

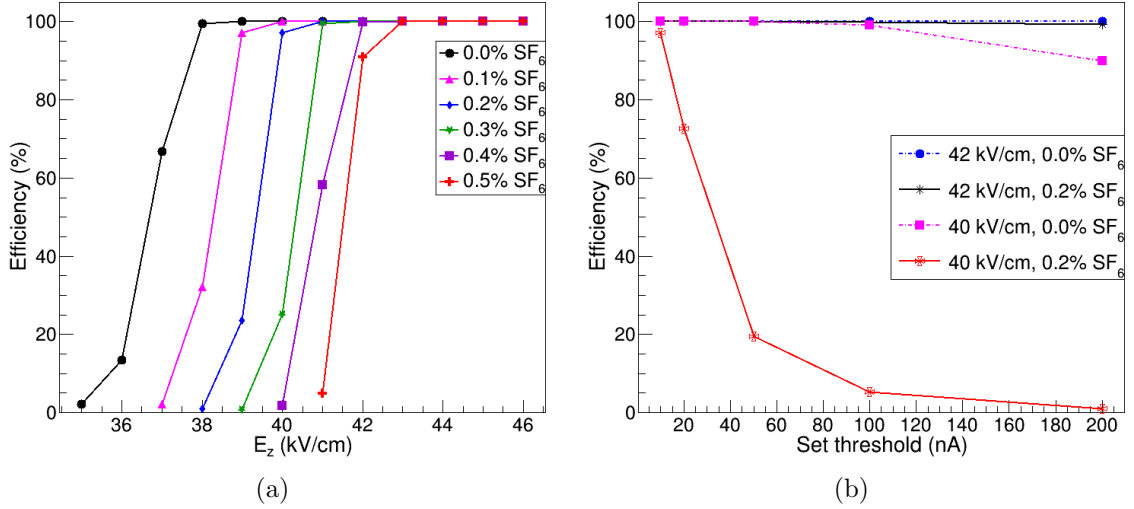


Figure 11: Variation of RPC efficiency with (a) the applied field for different fractions of SF₆ in the gas mixture, containing 5% i-C₄H₁₀ and rest C₂H₂F₄ (set threshold = 10 nA), (b) the set threshold for two different fields for the gas mixtures containing C₂H₂F₄, 5% i-C₄H₁₀ and variable fractions of SF₆.

the highest efficiency is achievable even when using a very high threshold (~ 200 nA). In experiments, a minimum field (or applied voltage) is required to have a signal amplitude crossing the discriminator threshold and producing a non-zero efficiency, which increases with the increase in the SF₆ fraction in the gas mixture.

4.2 Effect of geometrical parameters

Due to the distorted field map near the edge, and button spacers [11] of the RPC, the transport properties of the electrons are different at those regions which in turn influences the signal generation and timing properties of the de-

tector at those regions. Muons of varying energy and direction have been passed through the RPC at different distances from the edge spacer and button spacer of the typical shape to find their effect on the timing properties. The variation of average signal generation time and the intrinsic time resolution at different distances from the edge spacer is shown in figure 12 for the application of two different fields and for gas mixtures containing two different fractions of SF_6 with 5% $i\text{-C}_4\text{H}_{10}$ and rest $\text{C}_2\text{H}_2\text{F}_4$. presence of large errors on the data points close to the edge and button spacers are due to less statistics as the signals from those regions are of less amplitude and very few of them are able to cross the set threshold. It is evident from figure 12 that the timing properties deteriorate

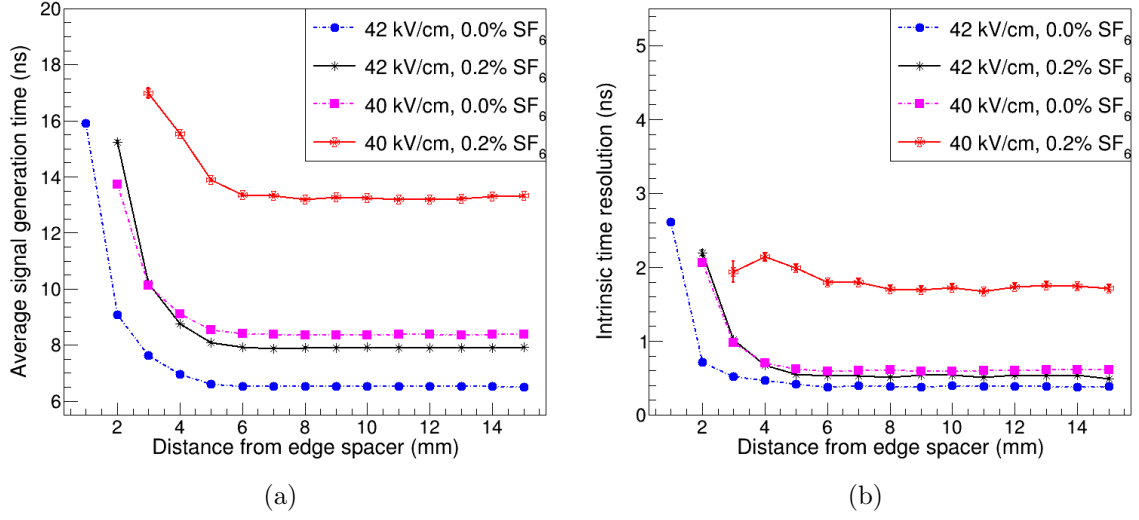


Figure 12: Variation of (a) average signal generation time and (b) intrinsic time resolution of a bakelite RPC near the edge spacer for different values of applied fields and different fractions of SF_6 in the gas mixture (used threshold = 10 nA).

very near to the edge spacer and the effect extends upto 5 mm from it. The variation of the same at different distances away from a button spacer is shown in figure 13. The button has a groove like structure, where the electric field is highly non-uniform and its value changes rapidly at the points within this non-uniform region [11]. This gives rise to a non-monotonic variation of the timing parameters in its close vicinity. From the figures 10, 12 and 13 it can be concluded that lower field and higher amount of SF_6 in the gas mixture worsen its timing performance.

The detector efficiency has been calculated at different distances away from the edge and button spacer of RPC by passing muons through those locations. The variation of efficiency with the distance from the edge spacer is shown in figure 14(a) for two different field values and different fractions of SF_6 in the gas mixture. The results obtained using a threshold of 10 nA are shown in solid lines whereas that using a threshold of -50 nA are shown in dotted lines in the same figure. For a fixed threshold, presence of higher amount of SF_6 in the gas mixture reduces the signal amplitude. Also operating the detector at lower field value has the same effect. These in turn produces a lower detection efficiency. Raising the value of used threshold decreases the number of events able to cross the threshold and in turn reduces the efficiency which is also visible in figure 14(a) for two different combinations of field and gas mixture. The electric field suffers near the spacers which is the reason for lower signal production in their

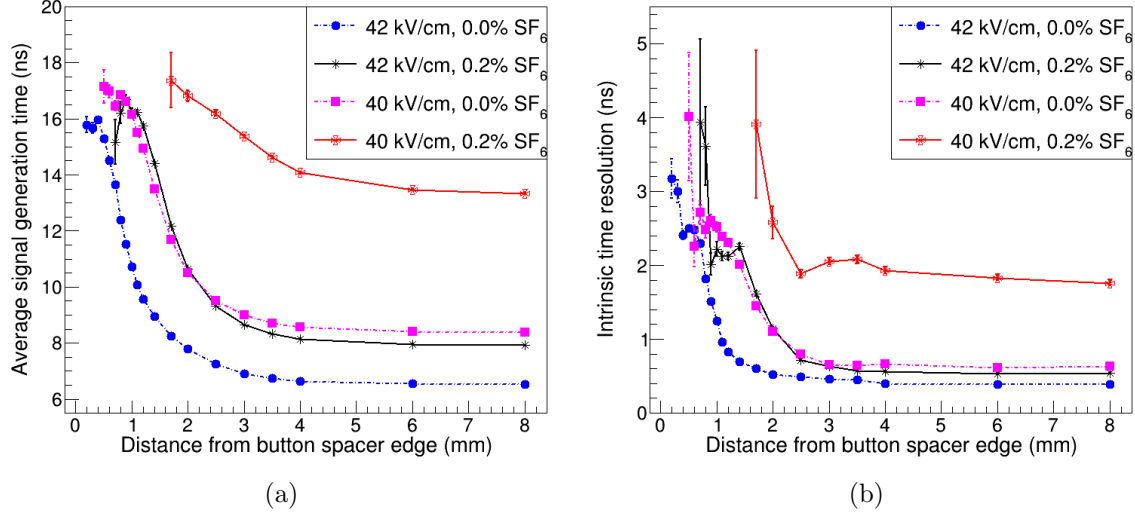


Figure 13: Variation of (a) average signal generation time and (b) intrinsic time resolution of a bakelite RPC near a button spacer for different values of applied fields and different fractions of SF₆ in the gas mixture (used threshold = 10 nA).

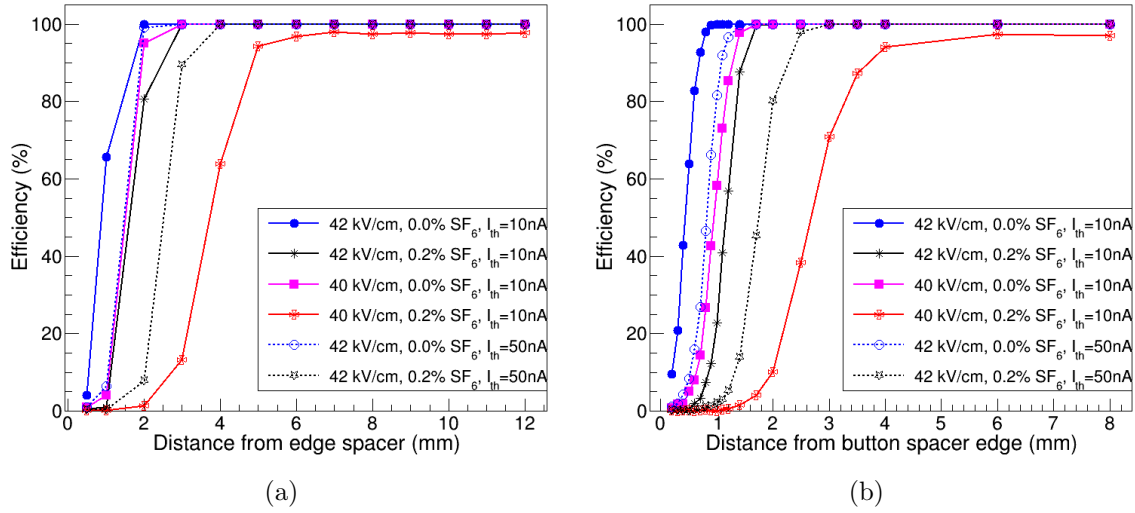


Figure 14: Variation of detector efficiency with the (a) distance from edge spacer, (b) distance from the edge of button spacer for different values of applied fields (40 kV/cm, 42 kV/cm) and different fractions of SF₆ (0.0%, 0.2%) in the gas mixture and for different used thresholds (10 nA, 50 nA).

vicinity. The variation of the detector efficiency with the distance from button spacer edge is shown in figure 14(b) where the same trend can be seen. The extent of the inefficient regions depend on the choice of applied field, used gas mixture and the set threshold. For the operation of the detector at 42 kV/cm with 0.2% SF₆, the inefficient region extends upto 3 mm from the edge spacer and about 1.75 mm from the button spacer if the used threshold is 10 nA. The inefficient region increases at higher threshold. A surface map of the detector efficiency in X-Y plane of an RPC with all its components is shown in figure 15 where $X = 0$ and $Y = 0$ are the boundaries between the gas chamber and the edge spacers. The map is generated for the RPC operated at 42 kV/cm with

the gas mixture containing 0.2% SF_6 and for the threshold of 10 nA. Effect of

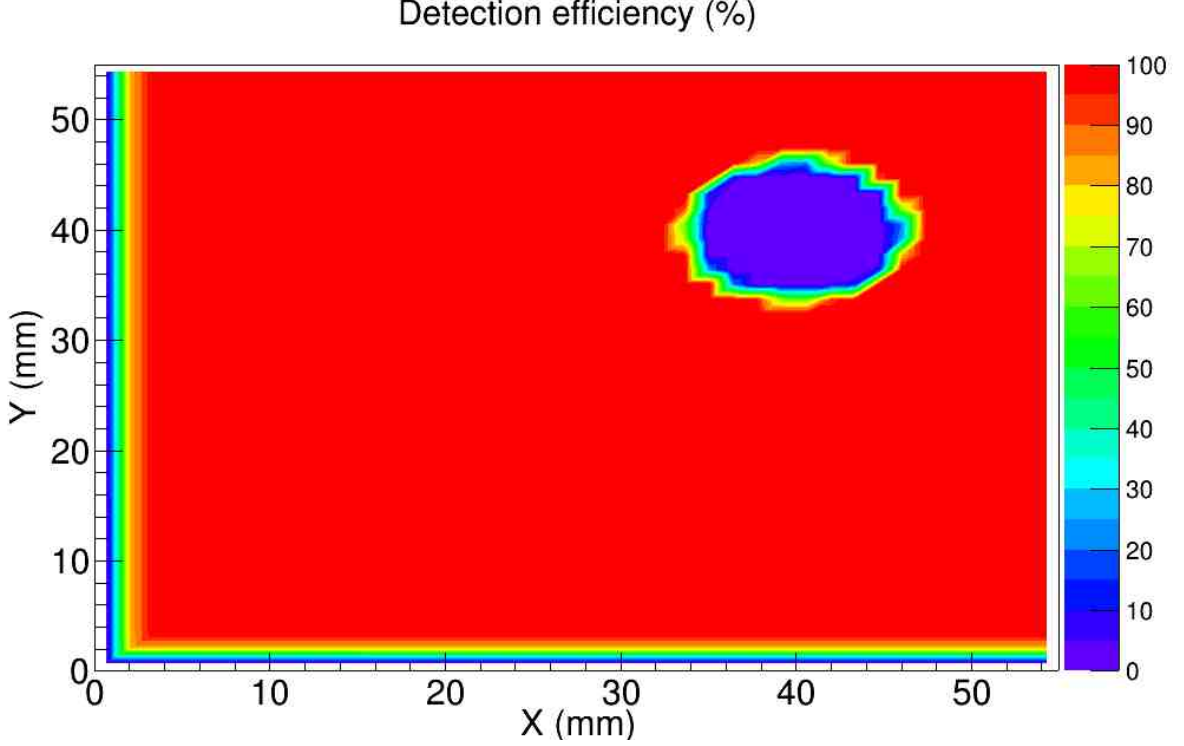


Figure 15: Surface map of RPC detection efficiency when it is operated with 94.8% $\text{C}_2\text{H}_2\text{F}_4$, 5% $i\text{-C}_4\text{H}_{10}$ and 0.2% SF_6 at 42 kV/cm (used threshold = 10 nA).

button spacer on the detection efficiency has been shown by placing a button spacer of stem radius 5.1 mm and paddle radius 5.5 mm with its center at $X = Y = 40$ mm. Similar kind of surface maps were found from experiments also [17, 18].

5 Computing resources

The calculations using Garfield have been performed in DELL PowerEdge R930 server having 256 GB RAM, 64 cores, 2.2 GHz CPU running CentOS 7.5. For fixed operating conditions, calculation of signals for the passage of 20000 muons, using field maps pre-calculated in neBEM and gas files prepared by Magboltz stand alone separately, takes 1 day 5 hours to complete.

6 Conclusion

The amplitude of the RPC signal increases with the increase in the applied voltage which in turn improves the efficiency of the detector. An RPC becomes faster with the increase in applied field (or voltage) and the time resolution also improves. However, raising the field to a very high value increases streamer probability [19] which is known to affect the RPC timing performance adversely. The electron quenching role of SF_6 is evident from the simulated results. Although a certain amount of SF_6 is used to limit the streamer generation, the increase of SF_6 proportion in the gas mixture deteriorates the timing performance

of the detector. So, to achieve the best timing performance in the avalanche mode operation with limited streamer contribution, a RPC is required to be operated at an optimum voltage along with an optimum amount of SF₆. From the above results operating an RPC of 2 mm gas gap containing 0.2% SF₆ at a field value of 42 kV/cm should be able to produce the best results.

The simulation predicts that the response of RPC at critical regions like very near to edge and button spacers gets altered due to the affected field map [11] at those regions. The timing response also gets affected adversely in those regions. The effect of these geometrical components vanish by about 7 mm away from edge spacers and about 5 mm away from the edge of the button spacers. So, the effective volume of RPC producing uniform response will be little less than the geometrical volume of its gas chamber. The detection efficiency also gets hampered near the spacers which in turn is expected to produce dead regions. The present robust simulation method can be used to find the timing performance of other gaseous detectors also, as well as their dependence on various operating and design parameters.

Acknowledgment

The financial support and the helpful review received from INO collaboration is gratefully acknowledged.

References

- [1] R. Santonico and R. Cardarelli, Development of resistive plate counters, *Nucl. Instr. Meth. A*, 187 (1981) 377.
- [2] A. Kumar, A. M. Vinod Kumar, A. Jash et al., Physics Potential of the ICAL detector at the India-based Neutrino Observatory (INO), *Pramana - J Phys.*, 88 (2017) 79.
- [3] M. Bhuyan et al., Development of 2 m × 2 m size glass RPCs for INO, *Nucl. Instr. Meth. A*, 661 (2012) S64-S67.
- [4] W. Shockley, Currents to conductors induced by a moving point charge, *Journal of Applied Physics*, 9 (1938) 635.
- [5] S. Ramo, Currents induced by electron motion, *Proceedings of the IRE.*, 27 (1939) 584.
- [6] R. Veenhoff, GARFIELD, recent developments, *Nucl. Instr. Meth. A*, 419 (1998) 726. <http://garfield.web.cern.ch/garfield>
- [7] I.B. Smirnov, *Modeling of ionization produced by fast charged particles in gases*, *Nucl. Instr. Meth. A*, 554 (2005) 474-493.
- [8] N. Majumdar and S. Mukhopadhyay, Simulation of 3D electrostatic configuration in gaseous detectors, *Journal of Instrumentation*, 2 (2007) P09006.
- [9] S.F. Biagi, *Accurate solution of the Boltzmann transport equation*, *Nucl. Instr. Meth. A*, 273 (1988) 533.
- [10] COMSOL Multiphysics® - multiphysics simulation tool, available at www.comsol.com.
- [11] A. Jash, N. Majumdar, S. Mukhopadhyay and S. Chattopadhyay, Numerical studies on electrostatic field configuration of Resistive Plate Chambers for the INO-ICAL experiment, *Journal of Instrumentation*, 10 (2015) P11009.

- [12] W. Riegler, Induced signals in resistive plate chambers, *Nucl. Instr. Meth. A*, 491 (2002) 258-271.
- [13] C. Lippmann and W. Riegler, Space charge effects in Resistive Plate Chambers, *Nucl. Instr. Meth. A*, 517 (2004) 54-76.
- [14] ROOT - Data Analysis Framework, available at root.cern.ch.
- [15] K. Raveendrababu, P. K. Behera, B. Satyanarayana, J. Sadiq, Study of glass properties as electrode for RPC, *Journal of Instrumentation*, 11 (2016) C07007.
- [16] W. Riegler and C. Lippmann, Detailed models for timing and efficiency in resistive plate chambers, *Nucl. Instr. Meth. A*, 508 (2003) 14.
- [17] M. Bhuyan et al., Cosmic ray test of INO PC stack, Figure 9, *Nucl. Instr. Meth. A*, 661 (2012) S68-S72.
- [18] A. D. Bhatt, V. M. Datar, G. Majumdar, N. K. Mondal, Pathaleswar and B. Satyanarayana, Improvement of time measurement with the INO-ICAL resistive plate chambers, *Journal of Instrumentation*, 11 (2016) C11001.
- [19] R. Cardarelli, V. Makeev, R. Santonico, Avalanche and streamer mode operation of resistive plate chambers, Figure 4, *Nucl. Instr. Meth. A*, 382 (1996) 470-474.